Design, Development, and Initial Testing of a Computationally-Intensive, Long-Endurance Solar-Powered Unmanned Aircraft

Or D. Dantsker[*], Mirco Theile[†], and Marco Caccamo[‡] — *University of Illinois at Urbana–Champaign, Urbana, IL 61801*

Renato Mancuso[§] — *Boston University, Boston, MA 02215*

In recent years, we have seen an uptrend in the popularity of UAVs driven by the desire to apply these aircraft to areas such as precision farming, infrastructure and environment monitoring, surveillance, surveying and mapping, search and rescue missions, weather forecasting, and more. The traditional approach for small size UAVs is to capture data on the aircraft, stream it to the ground through a high power data-link, process it remotely (potentially off-line), perform analysis, and then relay commands back to the aircraft as needed. All the mentioned application scenarios would benefit by carrying a high performance embedded computer system to minimize the need for data transmission. A major technical hurdle to overcome is that of drastically reducing the overall power consumption of these UAVs so that they can be powered by solar arrays. This paper describes the work done to date developing the 4.0 m (157 in) wingspan, UIUC Solar Flyer, which will be a long-endurance solar-powered unmanned aircraft capable of performing computationally-intensive on-board data processing. A mixture of aircraft requirements, trade studies, development work, and initial testing will be presented.

Nomenclature

CG	=	center of gravity
DOF	=	degree of freedom
ESC	=	electronic speed controller
GPS	=	global navigation satellite system
IMU	=	inertial measurement unit
IR	=	infrared
L/D	=	lift-to-drag ratio
PWM	=	pulse width modulation
RC	=	radio control
AR	=	aspect ratio
b	=	wingspan
c	=	wing mean chord
g	=	gravitational acceleration
L	=	aircraft length
m	=	aircraft mass
P	=	power
p, q, r	=	roll, pitch and yaw rates
S	=	wing area
W	=	weight
v	=	velocity

[*]Graduate Research Fellow, Department of Aerospace Engineering, AIAA Student Member. dantske1@illinois.edu
[†]Research Scholar, Department of Computer Science. mircot@illinois.edu
[‡]Professor, Department of Computer Science. mcaccamo@illinois.edu
[§]Assistant Professor, Department of Computer Science. rmancuso@bu.edu

α = angle of attack
η = efficiency
ϕ, θ, ψ = roll, pitch and heading angles

I. Introduction

In recent years, we have seen an uptrend in the popularity of UAVs driven by the desire to apply these aircraft to areas such as precision farming, infrastructure and environment monitoring, surveillance, surveying and mapping, search and rescue missions, weather forecasting, and more. The traditional approach for small size UAVs is to capture data on the aircraft, stream it to the ground through a high power data-link, process it remotely (potentially off-line), perform analysis, and then relay commands back to the aircraft as needed.[1–5] Given the finite energy resources found onboard an aircraft (battery or fuel), traditional designs greatly limit aircraft endurance since significant power is required for propulsion, actuation, and the continuous transmission of visual data. All the mentioned application scenarios would benefit by carrying a high performance embedded computer system to minimize the need for data transmission. Figure 1 shows the power consumption break down for a long-endurance UAV with a high performance computational platform onboard.

A major technical hurdle to overcome is that of drastically reducing the overall power consumption of these UAVs so that they can be powered by solar arrays. The process of reducing aircraft power consumption is required to reduce the aircraft weight, prolong flight time, and ultimately reduce cost in order to support the widespread adoption of UAVs for different types of missions. There have been many existing aircraft that use solar panels and are able to sustain flight during all daylight hours, however, lack the ability to perform significant on-board computation beyond automating flight.[6–10] On the other hand, there are several existing aircraft that use solar panels and batteries and are able to perform a variety of on-board tasks;[11,12] however, lack the ability to sustain flight during all daylight hours.

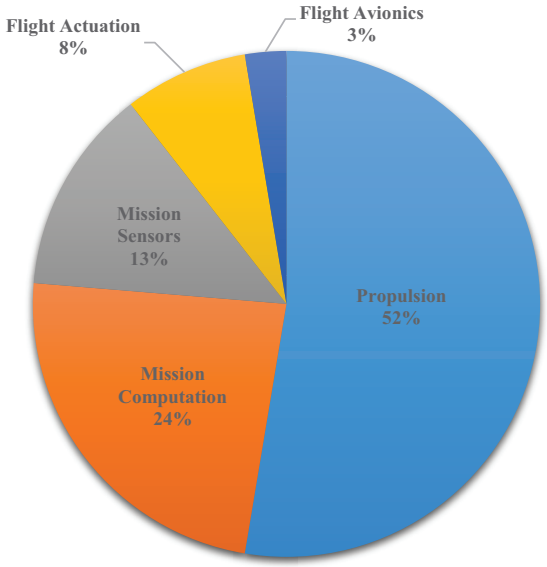

Figure 1. Breakdown of power consumption on computationally intensive UAV based on sizing and experimental data collected.

This paper describes the design, development and initial testing done to date of the UIUC Solar Flyer, a long-endurance solar-powered unmanned aircraft capable of performing computationally-intensive on-board data processing.[13] The aircraft, built from a majority of commercial-off-the-shelf components, was designed using a mixture of trade studies and power simulations in order to enable a variety of all-daylight hour missions while minimizing aircraft size. The completed 4.0 m (157 in) wingspan UIUC Solar Flyer aircraft will weight approximately 2.5 kg (88 oz) and have continuous daylight ability to acquire and process high resolution visible and infrared imagery. The aircraft will be instrumented with an integrated autopilot and high-fidelity data acquisition system as well as a dedicated graphics processing unit (GPU). The aircraft will be powered by a 65 W gallium arsenide (GaAs) solar array from Alta Devices. The aircraft configuration, wing platform area, and expected lift-to-drag ratio were also considered along with motor and propeller data.

This paper will first define the requirement for the UIUC Solar Flyer. Then, the paper will present two trade studies, which were indispensable in defining the aircraft design. After that, the paper will provide details of the development of the UIUC Solar Flyer along with specification of the aircraft, instrumentation, computational, and solar power systems. Next will be a description of the initial flight testing done to date including an example time history of un-powered gliding used to define the lift-to-drag ratio of the aircraft. Finally, a summary and future work will be provided.

II. Requirements

The design of the UIUC Solar Flyer was guided by a set of underlying requirements with the overarching goal to create a long-endurance solar-powered unmanned aircraft capable of performing computationally-intensive on-board data processing. Refining the design involved separating the aircraft requirements into two aspects: solar powered flight and sensor payload.

A. Solar Powered Flight

For the aircraft to fly from sunrise to sunset, it must be power self-sustaining. This means that, on average, the solar arrays on the aircraft must be able to produce as much electricity as is consumed. However, there may be times that the aircraft components need to consume more power than the solar arrays can generate, e.g. during takeoff or ascents. In those cases, an on-board battery system will be used to buffer the energy needed for peak demand.

With the assumption that the maximum number of solar cells permissible will be mounted onto the aircraft, an upper limit to the power produced by the solar array can be deduced from the manufacturer data sheet. However, the power produced by the solar array in flight will be lower than the ideal upper limit due to several factors, primarily: relative aircraft-sun orientation and cloud cover. Therefore, the design of the aircraft must conservatively take into account non-ideal solar power production expectations. Similarly, during flight, the allotment of power to aircraft components must vary in real-time based on the current and prediced future power production. Thus, propulsion system usage, affected by flight path and speed, and computational usage will need to adapt based on aircraft orientation, sun location (azimuth and elevation based on time and location), and cloud cover.

B. Sensor Payload

Based on the desired civilian applications, i.e. precision farming, infrastructure and environment monitoring, surveillance, surveying and mapping, search and rescue missions, weather forecasting, etc., the UIUC Solar Flyer must be able to support a variety of sensors. It was determined that the testbed aircraft developed should be able to support at least 2 visible light cameras as well as at least one infrared camera. Supporting these cameras comes in several forms: computation, power, and physical.

As an underlying goal of this research is to perform computation on-board and only transmit processed results to the ground, the avionics on-board must be able to process the visual data streams from the cameras. More specifically, this visual on-board computation ability comes in the form of equipping the aircraft with a dedicated graphics processing unit in addition to the flight control system. This dedicated graphics processing unit would actively process the visual data generated by the cameras, however, per the previous section, may need to be powered down depending on available power. Additionally, it is important to mention that the cameras will also require power and can also be powered down if needed.

The cameras and graphics processing unit will need to be physically present on the aircraft meaning they require mounting accommodations and wiring. The cameras, graphics processing unit, mounts, and wiring will increase the aircraft weight and therefore extra lift will need to be generated. The extra lift required will not only increase the propulsion power needed to maintain the same flight but may also decrease the airframe aerodynamic efficiency (due to the increased and non-ideal operating angle-of-attack). All of these factors need to be considered when evaluating which airframe is appropriate to use.

III. Trade Studies

The UIUC Solar Flyer design was refined with the use of trade studies to first establish general feasibility followed by an airframe comparison of possible sailplanes.

A. Preliminary Feasibility

For the study, a 3 m wingspan electric-propelled sailplane will be used as it has minimal drag. Based on Section II.B, the aircraft should be able to support two visible light cameras, one infrared camera, and a dedicated graphics processing unit. Presumably, these components should roughly consume between 5 and 20 W, depending on the computational load and device utilization[a]. Additionally 5 W should be allocated for flight instrumentation necessary for autopilot flight and data acquisition.

For the purpose of the study, it is also assumed the aircraft has a flight weight of 1.8 kg, a cruise speed of approximately 15 m/s, 70% efficient propulsion system, and an estimated lift-to-drag ratio of approximately 25. Given these values and the equation for power required in level flight,

$$P = \frac{WV}{\eta_{propulsion} \cdot L/D} \tag{1}$$

the aircraft would require approximately 15 W of power to maintain level flight. This is on the same order as the power consumed by the computational platform and thereby a careful power budget optimization and a reactive adaptation of computational resources are both crucial and justified.

The generic study aircraft was designed to be powered by a lithium polymer battery weighing approximately 400 gr. Given the earlier results, it is assumed that the aircraft would in total consume a continuous average of 40 W for propulsion, actuation, computation, and communication[b] in cruise under full computational load. Given a conservative lithium polymer battery energy density of 100 W-hr/kg, the aircraft would be expected to have an endurance of 1 hr. However, if the stock battery were to be replaced with a smaller battery, the difference in weight could be reallocated to install an array of solar cells that would supply a given power from an unlimited pool of energy during daylight hours. Light weight solar cells, such as those manufactured by Alta Devices,[17] produce approximately 1 W of power per installed gram of photovoltaic cell. Thus in order to power the aircraft in cruise under full computational utilization would only require 40 gr of solar cell to be installed. A 40 gr reduction in the lithium polymer battery used would correlate in a 6 min loss in battery powered endurance in exchange for continuous 40 W solar energy collection. The resultant aircraft would then have the capability to cruise for all daylight hours of the day plus 54 min[c].

It is important to highlight that an aircraft does not only cruise as there are flight segments that require more power, such as maneuvering and climbing, and less power such as gliding. Proper system-wide power management must be performed given that the aircraft is limited to using a relatively fixed amount of power at all times, in this case 40 W, per the power produced by 40 gr of solar panels during optimal daylight hours. During high propulsion power flight, the power used for computation must be decreased, while during low propulsion power flight, excess power can be allocated for computation or could otherwise be used to recharge the lithium polymer battery. During daylight hours, the lithium polymer battery would act as a large energy buffer to supplement the solar cells during peak power consumption time periods. Once daylight is no longer available, the battery acts as the sole energy provider.

In order to illustrate the significant benefit of using solar cells it is important to look at the performance expected from battery-only powered unmanned aircraft. Figure 2 shows the average power consumption, normalized to a 25 W,

[a]The visible and IR cameras were proposed in this early study to illustrate the feasibility of building a long-range UAV using COTS sensors for survey and surveillance missions. If a larger, custom-built 5-8 m motor-glider were used (presumably, with a higher L/D of 30-40); larger, heavier and more power consuming sensors could be used - these could include: Synthetic Aperture Radar (e.g. iMSAR NanoSAR, 910 g, 15 W[14]), Ground Penetrating Radar (e.g. Sterling Lightweight GPR, 990 g, 7 W[15]), and LIDAR (e.g. Velodyne Puck LITE, 590 g, 8 W[16]).

[b]In this early feasibility study, it is assumed that there would be substantially reduced radio usage since proposed UAV will be fully autonomous and its sensed data streams will be processed onboard, thereby minimizing the need for continuous communication, which would save a considerable amount of power.

[c]Notice that flight time is not considerably affected by environmental factors, most notably wind, yet there would be a decrease in ground speed of the aircraft and thus its range.

200 g payload plotted against the flight time for existing battery powered unmanned aircraft.[1,3–5,18–22] A trend line was plotted on the same figure that gives an estimate for the average power consumption of an aircraft as a function of the flight time, both of which were derived by the battery size. The average power consumption and flight time were calculated based on a field-able lithium polymer battery energy density of 0.576 MJ/kg, an aircraft lift-to-drag ratio of 20, an average flight speed of 20 m/s, and an empty aircraft weight equal to 2.7 times the weight of the battery and 200 gr payload. The trend line shows an exponential increase of the average propulsion power needed to sustain flight for longer flight times. The existing aircraft data points also show a significant increase in system cost with flight time. There are several existing aircraft that use solar panels and batteries;[7,11,12] however, they lack the ability to perform onboard real-time computation and more importantly, to sustain flight during all daylight hours.

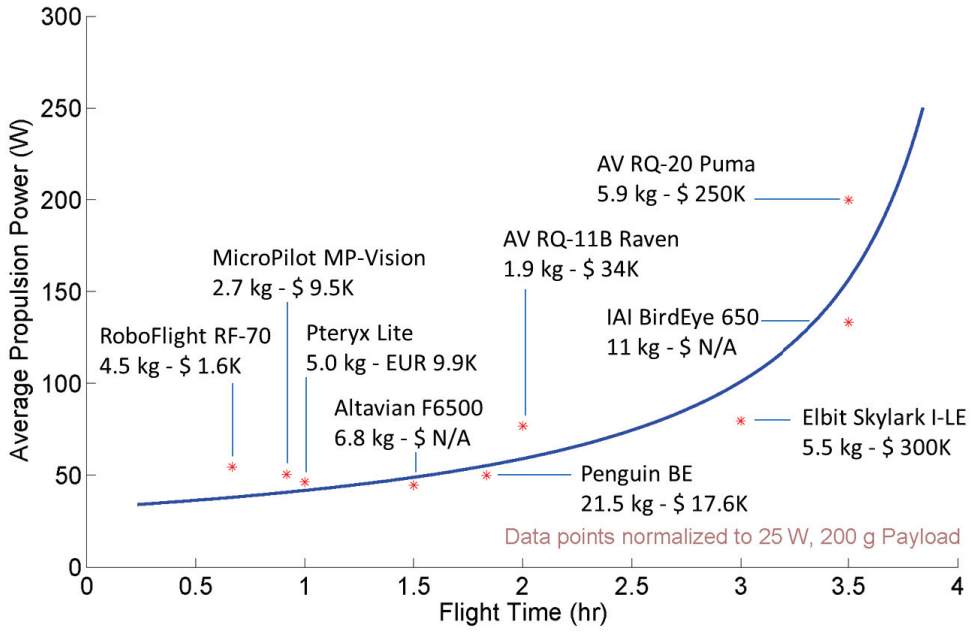

Figure 2. Propulsion power consumption vs. flight time for an generic electric aircraft with a 200 g, 25 W payload and for existing electric UAVs with their average propulsion power normalized per the payload power and mass.

B. Airframe Selection

Designing and building a custom airframe for the UIUC Solar Flyer is impractical in terms of both time and cost allotted for the research. There are many RC model airframes available that could be used. It was decided early on that given the mission, the airframe must have a high aspect ratio as this type of design provides maximum aircraft efficiency. A list of possible airframes was compiled and, using a variety of estimation methods (see below), their performance was compared.

Of the many airframes available, the airframes considered had to have wingspan of greater than or equal to 3 meters and be available for purchase at the start of the project. This led to two manufactures: F5 Models[d][24] and Top Model CZ.[25] Table 1 provides specifications for each of the possible airframes, as reported by the manufacturers. Figure 3 shows photos of each of the aircraft.

In order to provide a fair comparison between airframes, several parameters were assumed and held constant between airframes. First, based on Section II.B, a payload would include two visible light cameras, one infrared camera, and a dedicated graphics processing unit. Additionally, the aircraft would also carry a flight control and data acquisition system as well as solar panels and MPPT solar charge controller. The specific choices for the components fitted onto

[d]F5 Models has previously provided airframes used for solar UAVs[6,23]

(a) F5 Models Pulsar 3.2E

(b) F5 Models Pulsar 3.6E

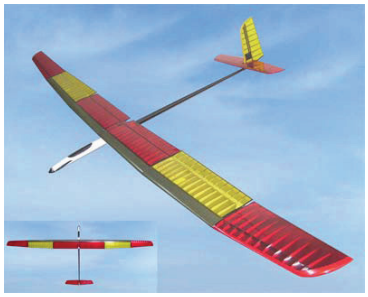

(c) F5 Models Pulsar 4E

(d) F5 Models Pulsar FPV

(e) Top Model CZ Samsara

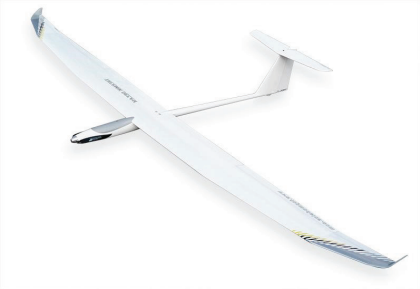

(f) Top Model CZ Thermik Dream

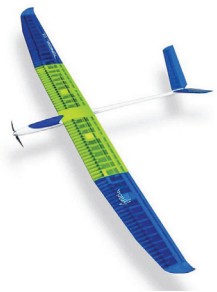

(g) Top Model CZ Gracia

(h) Top Model CZ Gracia MAXI

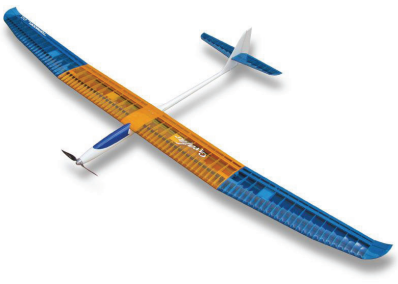

(i) Top Model CZ Grafas

(j) Top Model CZ Grafas MAXI

Figure 3. Photos of possible airframes (taken from F5 Models[24] and Top Model CZ[25]).

Table 1. Specifications of possible airframes.

Aircraft	Length [m]	Airfoil	Wingspan [m]	Wing Area [dm^2]	Average Chord [mm]	Aspect Ratio	Mass$_{flight}$ [gr]	Mass$_{bare}$ [gr]
F5 Models Pulsar 3.2E	1.73	AG25	3.20	70.5	220	14.5	1850	900
F5 Models Pulsar 3.6E	1.73	AG25	3.60	80.5	224	16.1	1950	1050
F5 Models Pulsar 4E	1.78	AG25	4.00	85.0	213	18.8	1980	1100
F5 Models Pulsar Twin	1.515	AG25	3.00	69.0	230	13.0	1980	1080
Top Model CZ Samsara	1.80	AG–	3.20	71.0	222	14.4	2155	1245
Top Model CZ Thermik Dream	1.51	S7012	3.00	60.9	203	14.8	2700	1940
Top Model CZ Gracia	1.51	MH32	3.07	70.5	230	13.4	2050	1245
Top Model CZ Gracia MAXI	1.51	MH32	3.52	80.1	228	15.5	2155	1305
Top Model CZ Grafas	1.54	MH32	3.07	70.5	230	13.4	2050	1300
Top Model CZ Grafas MAXI	1.54	MH32	3.52	80.1	228	15.5	2155	1420

the aircraft, their mass, and power requirements can be found in Table 2. Based on the components, an addition of 250 gr would be added onto each airframe and 20 W must be allocated to the mission components.

Table 2. Specifications of aircraft instrumentation and computational components chosen for airframe comparison.

Component	Mass [gr]	Power Requirement [W]	Use
Al Volo FC+DAQ	75	5	Flight control and data acquisition system
Nvidia TX1 w/Daughter	144	10	Dedicated graphics processing unit
Sony FCB-MA130	2.2	0.73	Visible light camera
FLIR Quark 2	30	3.3	Infrared camera

It was assumed that the solar panels would only be fitted onto the wings of the aircraft and would have 60% area coverage (it would be impractical to mount solar panels onto the control surfaces or leading edge). Based on the datasheet for Alta Devices single-junction GaAs solar cells,[26] a mass density of 150 gr/m^2 (assumed based on reported unshingled mass density of 114 gr/m^2) and solar power density of 260 W/m^2 were used; it was assumed that average real-life conditions would yield 50% the power of the ideal conditions in the data sheet (AM1.5, 1000 W/m^2, 25C) primarily due to relative orientation. Therefore, the mass of the solar array and the solar power produced for each airframe could be calculated as such:

$$m_{SolarArray} = 150gr/m^2 \times 60\% \times S \tag{2}$$

and

$$P_{SolarArray} = 260W/m^2 \times 50\% \times 60\% \times S \tag{3}$$

Table 3 summarizes the the possible area, mass and power of the solar arrays that could be fitted onto each of the possible airframes.

Finally, for the comparisons, steady level flight was assumed. The airframes considered will have different lift-to-drag ratios, however, as a first order approximation, a lift-to-drag ratio of 25 was used for all airframes. It was assumed that all aircraft will fly at a velocity of 20 m/s and that propulsion system efficiency will be between 50 and 65%. Therefore, the power required for flight would be:

$$P = \frac{(m_{flight} + m_{SolarArray} + m_{Components})g \cdot v}{\eta_{propulsion} \cdot L/D} \tag{4}$$

Table 3. Permissible solar array area, mass, and power for each of the possible airframes.

Aircraft	Solar Area [dm^2]	Solar Area Mass [gr]	Solar Power [W]
F5 Models Pulsar 3.2E	42.3	63.5	55.0
F5 Models Pulsar 3.6E	48.3	72.5	62.8
F5 Models Pulsar 4E	51	76.5	66.3
F5 Models Pulsar Twin	41.4	62.1	53.8
Top Model Samsara	42.6	63.9	55.4
Top Model Thermik Dream	36.54	54.8	47.5
Top Model CZ Gracia	42.3	63.5	55.0
Top Model CZ Gracia MAXI	48.06	72.1	62.5
Top Model CZ Grafas	42.3	63.5	55.0
Top Model CZ Grafas MAXI	48.06	72.1	62.5

The results of the airframe comparison is provided in Table 4. Of the possible airframes, the F5 Models Pulsar 4E had the greatest remaining power available to be used for the components. The Pulsar 4E had the greatest wingspan and wing area while having one of the lowest non-instrumented, flight-ready mass. This will allow for maximum solar power to be generated while minimizing the power required to propel the base airframe. Additionally, it is important to mention that the remaining power will not only be allocated to the components but also the propulsion system for manuevers that require more power than steady level flight, e.g. takeoffs, ascents, and turns.

Table 4. Power available for components on possible airframes.

Aircraft	Total Mass [gr]	Thrust Power [W]	Propulsion Power Required [W] $\eta = 65 - 50\%$	Solar Power Available [W]	Power Available for Components [W] $\eta = 65 - 50\%$
F5 Models Pulsar 3.2E	2167	17.0	26.2 – 34.0	55.0	28.8 – 21.0
F5 Models Pulsar 3.6E	2276	17.9	27.5 – 35.7	62.8	35.3 – 27.1
F5 Models Pulsar 4E	2310	18.1	27.9 – 36.3	66.3	38.4 – 30.0
F5 Models Pulsar Twin	2296	18.0	27.7 – 36.0	53.8	26.1 – 17.8
Top Model Samsara	2472	19.4	29.9 – 38.8	55.4	25.5 – 16.6
Top Model Thermik Dream	3008	23.6	36.3 – 47.2	47.5	11.2 – 0.3
Top Model CZ Gracia	2367	18.6	28.6 – 37.2	55.0	26.4 – 17.8
Top Model CZ Gracia MAXI	2480	19.5	29.9 – 38.9	62.5	32.5 – 23.5
Top Model CZ Grafas	2367	18.6	28.6 – 37.2	55.0	26.4 – 17.8
Top Model CZ Grafas MAXI	2480	19.5	29.9 – 38.9	62.5	32.5 – 23.5

IV. Development

The development of the UIUC Solar Flyer is separated into several categories: airframe, instrumentation, computation and sensing, and solar.

A. Airframe

The UIUC Solar Flyer airframe was built from a majority of commercial-off-the-shelf components. The structure was assembled from a F5 Models Pulsar 4.0E Pro electric model sailplane, which was chosen among a variety of other aircraft, per the trade study in Section III.B. The airframe fuselage is composed of a kevlar fuselage pod and a carbon fiber tail boom. All of the flight surfaces are built from balsa wood that is reinforced with carbon fiber and a kevlar-carbon fiber laminate. The wings are composed out of 3 sections: center with flaps and outer right and left with ailerons; Figure 4 shows the construction of the outer right wing section and the servo actuator linkage connected to the aileron. The tail has a vertical stabilizer with a rudder, which makes up a majority of the chord, and full-moving horizontal stabilizer; the tail can be seen in Figure 5.

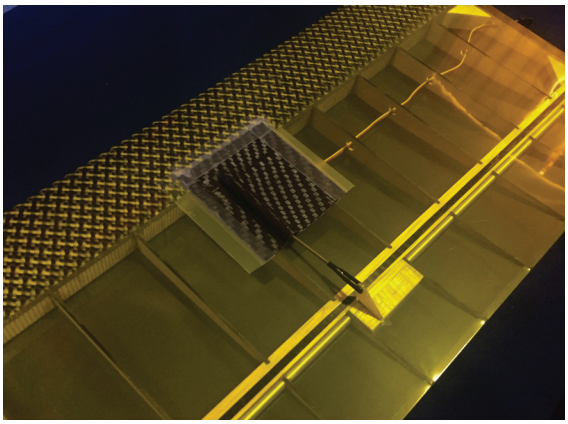

Figure 4. The outer right wing section of the UIUC Solar Flyer airframe, with servo actuator linkage connecting to the aileron.

Figure 5. The tail of the UIUC Solar Flyer airframe, with a full-moving horizontal stabilizer.

The airframe was built per the manufacturer instructions with some slight modifications to increase aircraft efficiency and ease future computational device and solar array integration. The only major deviation from the manufacturer specifications was the combination of the motor and propeller used. The choice of motor and propeller was made using propulsion and power simulations[27,28] and yielded the highest efficiency propulsion system possible from hundreds of possible permissible combinations for the aircraft parameters and expected flight envelope, i.e. flight velocities and thrust requirements. Figure 6 shows propulsion system as seen from the rear of the aircraft without the battery.

The final physical specifications for the instrumented, non-solar aircraft are given in Table 5. The specifications of the components used in the construction of the airframe is provided in Table 6. A photo of the completed flight ready airframe can be seen in Figure 7. It is noteworthy to mention that the airframe, flight-ready with the instrumentation integrated, had a final mass of 1966 gr, which is within the flight-ready weight provided by the manufacturer for a standard RC model.

Figure 6. The propulsion system of the UIUC Solar Flyer airframe, as seen from the rear of the aircraft.

Figure 7. The completed flight-ready, instrumented (non-solar) UIUC Solar Flyer airframe.

Table 5. Instrumented (non-solar) aircraft physical specifications.

Geometric Properties	
Overall Length	1815 mm (71.5 in)
Wing Span	4000 mm (157.5 in)
Wing Area	85 dm^2 (1318 in^2)
Aspect Ratio	18.8
Inertial Properties	
Gross Weight	1.966 kg (4.33 lb)
Empty Weight	1.739 kg (3.83 lb)
Wing Loading	23.1 gr/dm^2 (7.57 oz/ft^2)

Table 6. Instrumented (non-solar) aircraft airframe component specifications.

Airframe	
Model	F5 Models Pulsar 4.0E
Construction	Fully-composite kevlar and carbon fiber fuselange and built-up balsa wood with carbon fiber and a kevlar-carbon fiber laminate reinforced flight surfaces.
Flight Controls	
Control Surfaces	(2) Ailerons, (2) elevator, rudder, (2) flap, and throttle
Transmitter	Futaba T14MZ
Receiver	Futaba R6208SB
Servos	(6) S3173SVi
Power	Castle ESC - BEC
Propulsion	
Motor	Model Motors AXi Cyclone 46/760
ESC	Castle Creations Phoenix Edge Lite 50
Propeller	Aeronaut CAM Folding 13x6.5
Motor Flight Pack	Thunder Power ProLiteX 3S 2800 mAh

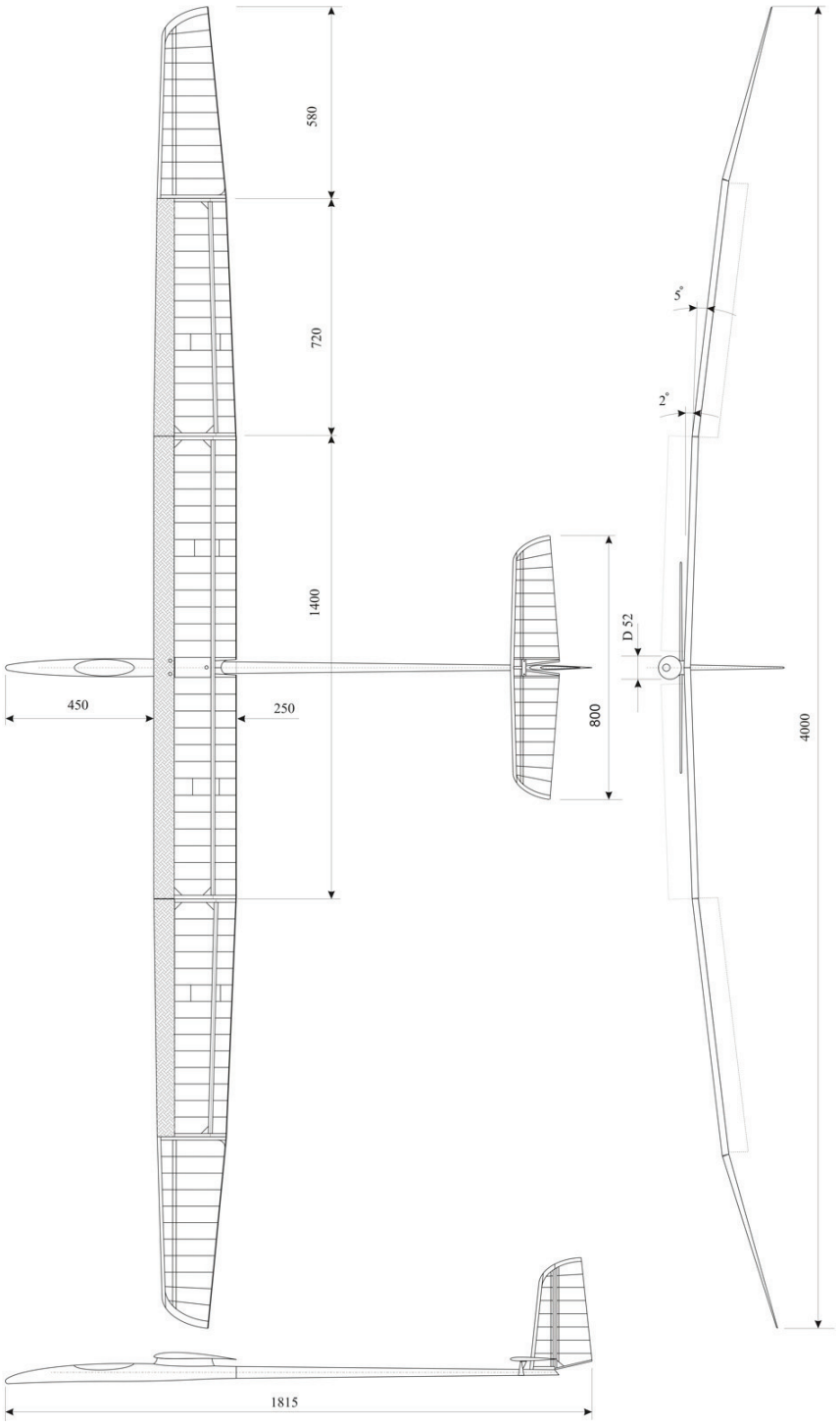

Figure 8. Dimensioned drawings of UIUC Solar Flyer airframe (taken from F5 Models[24]).

B. Instrumentation

The UIUC Solar Flyer was instrumented with an Al Volo FC+DAQ flight control and data acquisition system. The specifications of the instrumentation are given in Table 7. A cross section illustration of the instrumentation layout of the fuselage pod is given in Figure 9 while a top-view photo of the fuselage pod is shown in Figure 10. A photo of the entire center wing panel showing instrumentation components and servo actuators can be found in Figure 11.

Table 7. Instrumentation specifications.

Autopilot-DAQ system	Al Volo FC+DAQ 100 Hz flight control and data acquisition system
RF Module	Digi International 900 MHz XBee Pro S3B Module
Multiplexer	8-channel custom PWM multiplexer with redundant input
Sensors	
Inertial	100 Hz AHRS integrated into FC+DAQ
Positioning	10 Hz GNSS integrated into FC+DAQ
Airspeed sensor	Al Volo Pitot Static Airspeed Sensor
Motor sensor	Al Volo Castle ESC Interface
Power	
Regulator	Built into FC+DAQ
Battery	Thunder Power ProLiteX 2S 500 mAh

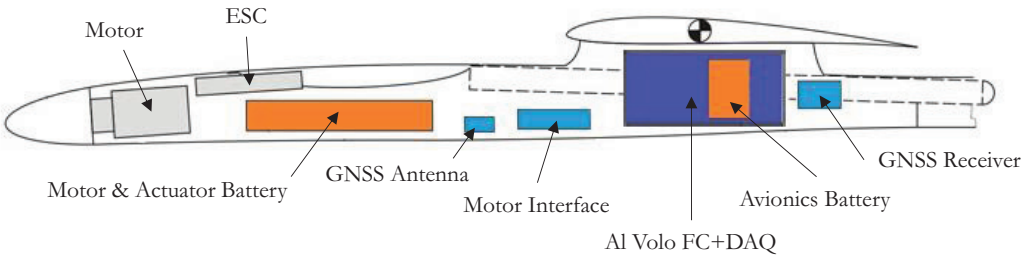

Figure 9. Internal layout of the fuselage pod showing Al Volo FC+DAQ flight control and data acquisition system in dark blue, the instrumentation sensors in blue, the batteries in orange, and the propulsion system in grey; the suggested center of gravity of the aircraft is also marked.

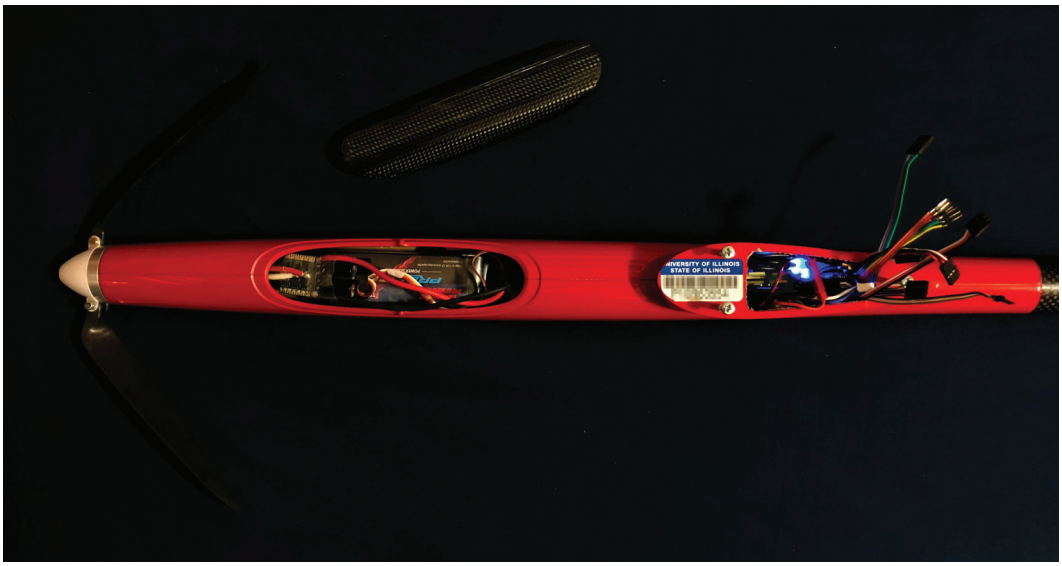

Figure 10. A photo of the top of the fuselage pod showing propulsion system elements in the front of the pod and the instrumentation in the rear of the pod; note that the wires connect to the sensors and flight control actuation system located in the wing.

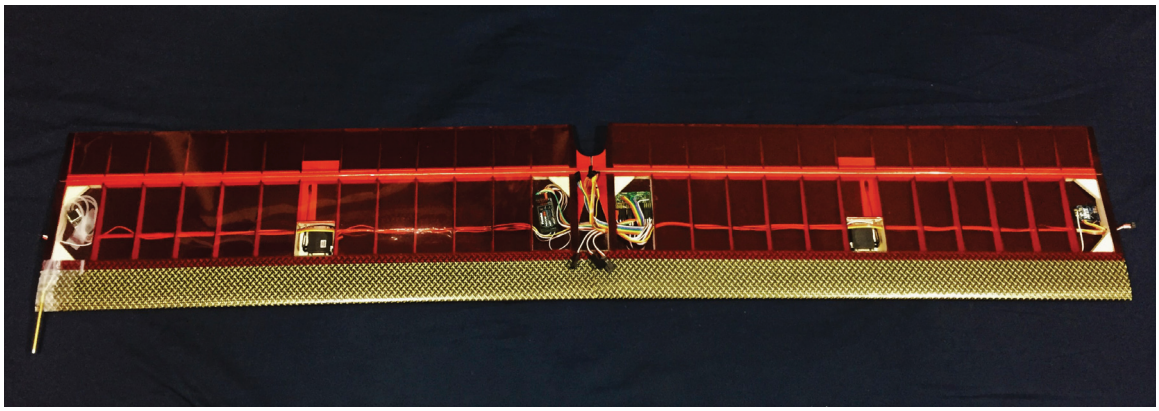

Figure 11. The center wing panel of the instrumented UIUC Solar Flyer airframe showing the instrumentation components and servo actuators.

The system operates at 100 Hz and has an integrated attitude and heading reference system (AHRS) / 9 degree-of-freedom (9-DOF) inertial measurement unit (IMU) and a 10 Hz Global Navigation Satellite System (GNSS) receiver among many other sensors. The system was stripped of its enclosure for this application and has a mass of approximately 70 gr. The Al Volo FC+DAQ was hard mounted into the rear of the fuselage pod such that the integrated AHRS would be aligned with the aircraft (with a 90 deg roll offset). The GNSS receiver was mounted nearby with the antenna being mounted forward in an area with minimal carbon fiber and thus minimal shielding.

Sensors were installed throughout the aircraft to perform various types of measurement. An Al Volo Pitot Static Airspeed Sensor was installed at the leading edge of the left tip of the center wing panel; the probe was attached to the skin of the aircraft using adhesive tape and the sensors and plumbing were installed in the nearby box section using double-sided adhesive tape. The airspeed probe and sensor can be seen in Figure 12. An Al Volo Castle ESC Interface was installed in the center of the fuselage pod between the ESC and the FC+DAQ. The sensor provides propulsion system data including system voltage, current, rotation rate (RPM per pulse), and throttle percentage.

Finally, support equipment for autopilot flight, i.e. a multiplexer and RF module, were installed in the wing of the aircraft along with the RC receiver required for manual flight. On the outer right end of the center wing section, a 900 MHz Digi XBee Pro RF module was installed to provide communication between the FC+DAQ and a ground station operator; this RF module can be seen in Figure 13. Then in the wing box just right of center, the multiplexer was mounted using hook and loop. The receiver was mounted on the opposite wing box section on the left, with PWM signal wires running between the two sides. The multiplexer outputs a set of wires to connect to the elevator and rudder servos in the fuselage as well as to the ESC. Additionally, the multiplexer also provides a set of wires to connect to the FC+DAQ in the fuselage for autopilot PWM signals to be routed. The center wing box area can be seen in Figure 14.

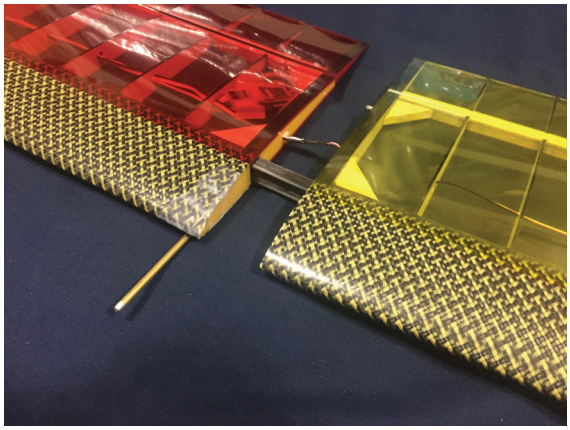

Figure 12. The Al Volo Pitot Static Airspeed Sensor installed at the leading edge of the left tip of the center wing panel.

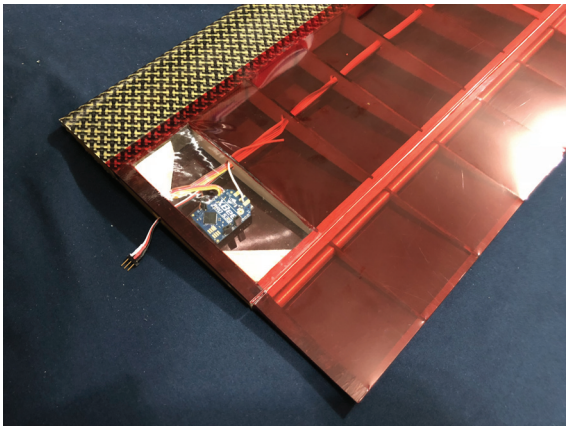

Figure 13. The 900 MHz Digi XBee Pro RF module installed in the wing box secion at the right end of the center wing panel.

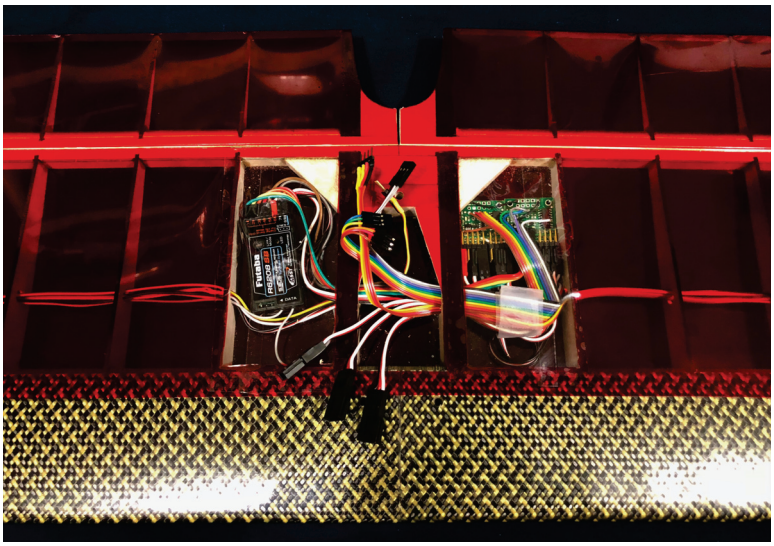

Figure 14. The center area of the wing where the multiplexer and RC receiver are mounted along with the wiring necessary for autopilot flight.

C. Computation and Sensing

To accommodate for potential missions, such as surveying and surveillance, the UIUC Solar Flyer will be equipped with two visual and one infrared camera. The data stream of the cameras will be processed by an Nvidia Tegra TX1. The components are listed in Table 8. Data processing computation tasks are usually highly parallelizable and can therefore take advantage of a GPU. Figure 15 shows a measurement of the power consumption of the Nvidia Tegra GPU in relation to the computational load. The measurements were conducted with a constant operating temperature of 40° C. The graphic shows an exponential relation between computational load and power consumption of the GPU as well as a peak power consumption of approximately 9 W.

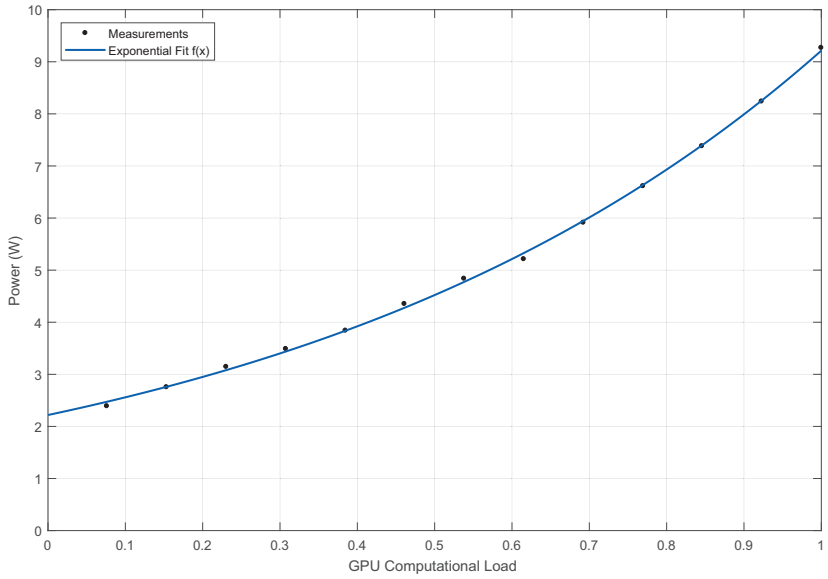

Figure 15. Tegra GPU power consumption in relation to computational load at a constant operating temperature of 40°*C*.

This load dependency of the power requirements of the GPU can be used for the system-wide power management during flight. When propulsion power consumption is low and solar generation is high, the computation can be ramped up. When flying into the wind or during low sun intensity times, the computational load can be reduced. As the control of the computational load can happen in an instant, the mission computation subsystem can be used to rapidly regulate the overall power consumption of the UIUC Solar Flyer, to react to environmental changes.

Table 8. Computational system and sensors specifications.

Graphics processing unit	Nvidia TX1
Sensors	
Visible camera	2x Sony FCB-MA130
IR camera	FLIR Quark 2
Power	
Regulator	Built into Nvidia TX1

D. Solar

The UIUC Solar Flyer will be powered by a single junction gallium arsenide (GaAs) solar array from Alta Devices.[17] Based on preliminary estimates the aircraft will be able to carry 65 W of solar cells mounted onto the upper surface of the wings. Areas such as the leading edge and the control surfaces will not have solar cells mounted on them due to the the overhead weight and wiring associated as well as the decreased solar power production potential.

Testing of the solar cells has been performed on a pan-tilt testing rig, which can be seen in Figure 16. The testing rig is able to precisely turn the solar cells and is equipped with an IMU and GPS such that the orientation and location, relative to the sun, can be measured. A MPPT solar charge controller, small 3-cell lithium polymer battery (similar to the battery on the aircraft), and load were also integrated into the test rig.

Figure 16. Solar cell and power management testbed.

V. Initial Testing

Initial flight testing was performed with the UIUC Solar Flyer in the spring of 2018. Up to date, a handful of manual flights were performed to parametrize the aircraft aerodynamic performance and power consumption characteristics. An example flight test segment that was performed to determine the best L/D of the aircraft can be seen in Figure 17. The figure shows rather smooth gliding flight with minimal perturbations. The human pilot reported that the aircraft is very sensitive to environmental conditions such as wind and thermal up-drafts, which makes capturing data manually difficult.

More testing is planned in the upcoming months using an automated flight sequencer, which is integrated into the Al Volo FC+DAQ flight control and data acquisition system using the uavAP autopilot[13] , and precisely steps the aircraft through a set of maneuvers that can be used to determine the aircraft parameters. By automating the data collection process, as opposed to manual flight, the aircraft parametrization and modeling process is performed with minimal trial-and-error and thus, more importantly, less flight time required. For example, by automating the flight testing process, aircraft inertial state variables such as pitch, roll, and velocity can be set and maintained during flight with greater accuracy than manual piloting. Preliminary automated flight data testing is being perfected in an emulation environment that has been used for previous research.[29,30]

VI. Summary and Future Work

This paper described the design, development and initial testing done to date of the UIUC Solar Flyer, which will be a long-endurance solar-powered unmanned aircraft capable of performing computationally-intensive on-board data processing. The aircraft was designed using a mixture of trade studies and power simulations in order to enable a variety of all-daylight hour missions while minimizing aircraft size. The completed 4.0 m (157 in) wingspan UIUC Solar Flyer aircraft is being built from a majority of commercial-off-the-shelf components, will weigh approximately 2.5 kg (88 oz), and will have continuous daylight ability to acquire and process high resolution visible and infrared imagery. The aircraft has been instrumented with an integrated autopilot and high-fidelity data acquisition system and will soon have a dedicated graphics processing unit (GPU) installed. The aircraft will be powered by a 65 W gallium arsenide (GaAs) solar array from Alta Devices, which is in the process of being built. Initial flight testing of the aircraft has been performed yielding preliminary aerodynamic performance characteristics.

More flight testing is planned in the near future to further determine the aircraft aerodynamic performance and power consumption characteristics. This flight testing will be performed using an automated flight sequencer that will be integrated into the autopilot. Next the dedicated graphics processing unit and cameras will be installed into the aircraft, flight tested, and characterized. Finally, the solar arrays will be integrated into the wing allowing for final flight testing to occur. Additionally, for the aircraft to reliably fly under environmental changes a system-wide power managment system will be developed and integrated into the uavAP autopilot.

Acknowledgments

The material presented in this paper is based upon work supported by the National Science Foundation (NSF) under grant number CNS-1646383. Any opinions, findings, and conclusions or recommendations expressed in this publication are those of the authors and do not necessarily reflect the views of the NSF.

The authors would like to thank Al Volo LLC for their generous loan of data acquisition equipment.

The authors would like to acknowledge Daniel Amir and Moiz Vahora for their support during the development and initial testing.

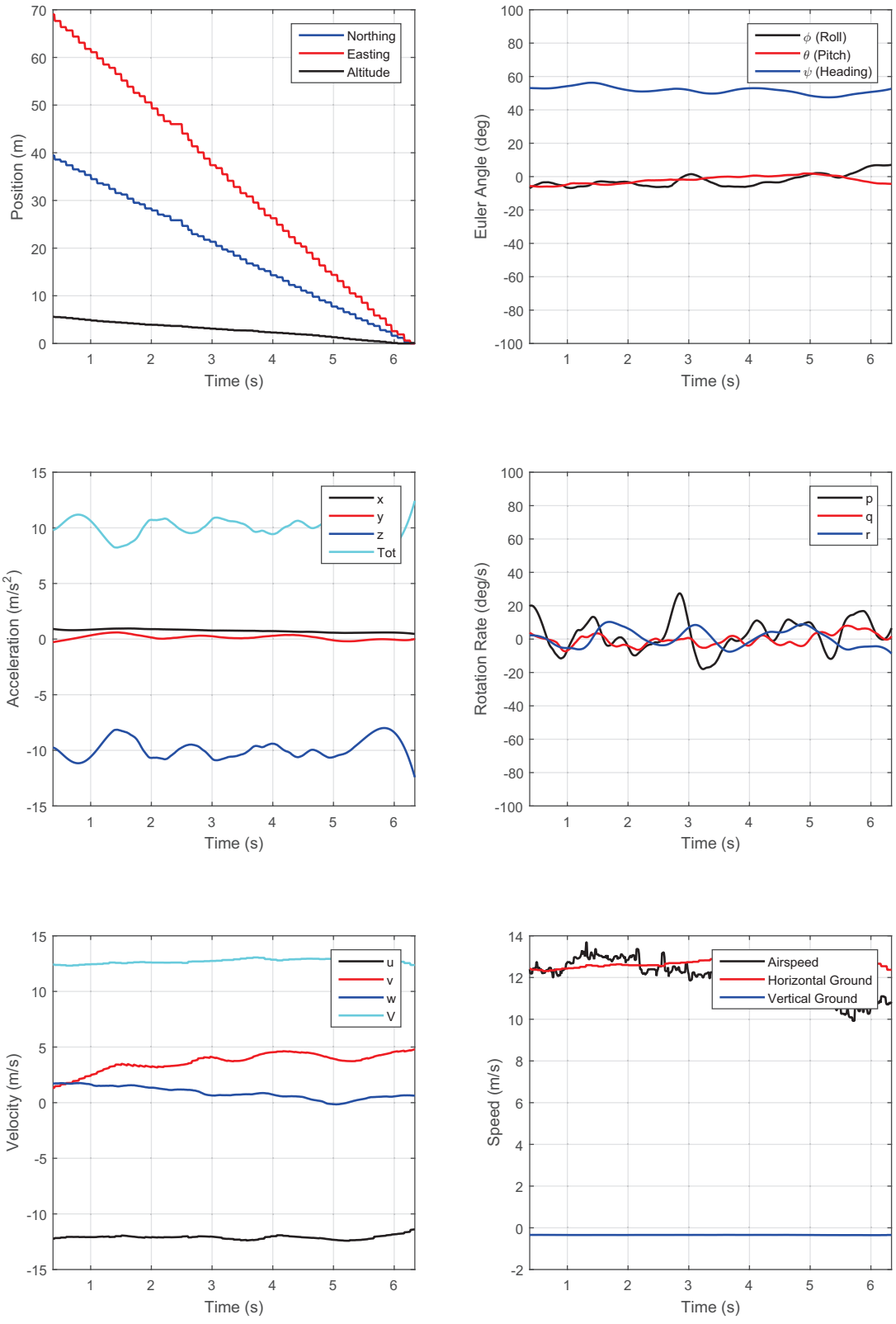

Figure 17. A time history of the instrumented UIUC Solar Flyer aircraft state during un-powered descent (glide) flight with a L/D ratio of approximately 34.

References

[1]Altavian, "Products - Altavian," http://www.altavian.com/Products, Accessed Apr. 2015.

[2]Precision Hawk, "Precision Agriculture, Commercial UAV and Farm Drones For Sale," http://precisionhawk.com/, Accessed Apr. 2015.

[3]Troy Built Models, "RoboFlight RF?70," http://www.troybuiltmodels.com/items/RF70-KIT.html, Accessed Apr. 2015.

[4]MicroPilot, "MicroPilot - MP-Vision," http://www.micropilot.com/products-mp-visione.htm, Accessed Apr. 2015.

[5]Trigger Composites, "Pteryx UAV," http://www.trigger.pl/pteryx/index.php, Accessed Apr. 2015.

[6]Ahn, I.-Y., Bae, J.-S., Park, S., and Yang, Y.-M., "Development and Flight Test of a Small Solar Powered UAV," Vol. 41, 11 2013.

[7]ETH Zurichs Autonomous Systems Lab, "Atlantik-Solar," http://www.atlantiksolar.ethz.ch/, Accessed Apr. 2015.

[8]Weider, A., Levy, H., Regev, I., Ankri, L., Goldenberg, T., Ehrlich, Y., Vladimirsky, A., Yosef, Z., and Cohen, M., "SunSailor: Solar Powered UAV," http://webee.technion.ac.il/people/maxcohen/SunSailorArt19nov06.pdf, Nov. 2006.

[9]Morton, S., D'Sa, R., and Papanikolopoulos, N., "Solar powered UAV: Design and experiments," *2015 IEEE/RSJ International Conference on Intelligent Robots and Systems (IROS)*, 2015, pp. 2460–2466.

[10]Betancourth, N. J. P., Villamarin, J. E. P., Rios, J. J. V., Bravo-Mosquera, P. D., and Ceron-Munoz, H. D., "Design and Manufacture of a Solar-Powered Unmanned Aerial Vehicle for Civilian Surveillance Missions," *Journal of Aerospace Technology and Management*, Vol. 8, 12 2016, pp. 385 – 396.

[11]Silent Falcon UAS Technologies, "Silent-Falcon sUAS," http://www.silentfalconuas.com/Silent-Falcon.html, Accessed Apr. 2015.

[12]AeroVironment, "AeroVironment Solar-Powered Puma AE Small Unmanned Aircraft Achieves Continuous Flight for More Than Nine Hours," http://www.avinc.com/resources/press-release/aerovironment-solar-powered-puma-ae-small-unmanned-aircraft-achieves-contin, Accessed Apr. 2015.

[13]Real Time and Embedded System Laboratory, University of Illinois at Urbana-Champaign, "Solar-Powered Long-Endurance UAV for Real-Time Onboard Data Processing," http://rtsl-edge.cs.illinois.edu/UAV/, Accessed Jan. 2018.

[14]Scannapieco, A. F., Renga, A., and Moccia, A., "Preliminary Study of a Millimeter Wave FMCW InSAR for UAS Indoor Navigation," *Sensors*, Vol. 15, No. 2, 2015, pp. 2309.

[15]Sterling Geo, "Lightweight GPR," http://www.sterlinggeo.com/assets/pdfs/SAL-CAS-300614-LightweightGPR-V9.pdf, Accessed Jun. 2016.

[16]Velodyne LiDAR, Inc., "Velodyne LiDAR Puck LITE," http://velodynelidar.com/docs/datasheet/63-9286$_{Rev-BPuckAccessedJun}$.2016.

[17]Alta Devices, "Solar powered UAV/UAS increases range and flight duration — Alta Devices," http://www.altadevices.com/applications-uavs.php, Accessed Apr. 2017.

[18]UAV Factory USA, LLC, "Penguin BE UAV Platform," http://www.uavfactory.com/prodcat/67, Accessed Apr. 2015.

[19]AeroVironment, "UAS: RQ-11B Raven," http://www.avinc.com/uas/small_uas/raven/, Accessed Apr. 2015.

[20]AeroVironment, "UAS: RQ-20A Puma," http://www.avinc.com/uas/small_uas/puma/, Accessed Apr. 2015.

[21]Elbit Systems Ltd. , " Skylark I LE - Mini UAS," https://www.elbitsystems.com/elbitmain/area-in2.asp?parent=3&num=279&num2=279, Accessed Apr. 2015.

[22]Israeli Aerospace Industries , "BirdEye 650 MINI UAS," http://www.iai.co.il/Sip_Storage//FILES/3/38203.pdf, Accessed Nov. 2015.

[23]Ahn, I.-Y., Yang, Y.-M., Ju, Y.-C., Park, S., and Bae, J.-S., "Efficiency Estimation on Propulsion System of an Electric Powered UAV," Vol. 23, 09 2015, pp. 1–7.

[24]"F5 Models," http://f5models.com, Accessed Oct. 2017.

[25]"Top Model CZ," https://www.topmodelcz.cz/, Accessed Oct. 2017.

[26]Alta Devices, "Technology Brief - Single Junction," https://www.altadevices.com/wp-content/uploads/2018/01/tb-single-junction-1712-001.pdf, Accessed Apr. 2018.

[27]Dantsker, O. D., Theile, M., and Caccamo, M., "A High-Fidelity, Low-Order Propulsion Power Model for Fixed-Wing Electric Unmanned Aircraft," AIAA/IEEE Electric Aircraft Technologies Symposium, Jul. 2018.

[28]Dantsker, O. D. and Caccamo, M., "Propulsion System Optimization of a Long-Endurance Solar-Powered Unmanned Aircraft," AIAA/IEEE Electric Aircraft Technologies Symposium, Jul. 2018.

[29]Theile, M., Dantsker, O. D., Nai, R., and Caccamo, M., "uavEE: A Modular, Power-Aware Emulation Environment for Rapid Prototyping and Testing of UAVs," Submitted to IEEE International Conference on Embedded and Real-Time Computing Systems and Applications, Hakodate, Japan, August 2018.

[30]Caccamo, M., Dantsker, O., and Theile, M., "uavEE: Unmanned Aerial Vehicle Emulation Environment for Rapid Prototyping of Embedded Software and Hardware," CPSWeek 2018 Tutorial, http://rtsl-edge.cs.illinois.edu/UAV/tutorial.html.